Investigations of thermal behaviours of asphalt pavement under short-term preheating technique for pavement overlay construction

Song, Xinyi; Sun, Lijun; Cheng, Huailei; Zhang, Hongchao; Han, Zhanchuang; Hu, Yue; Li, Yi

DOI
10.1080/10298436.2024.2443666

Publication date
2024

Document Version
Final published version

Published in
International Journal of Pavement Engineering

Citation (APA)
Song, X., Sun, L., Cheng, H., Zhang, H., Han, Z., Hu, Y., & Li, Y. (2024). Investigations of thermal behaviours of asphalt pavement under short-term preheating technique for pavement overlay construction. *International Journal of Pavement Engineering*, *25*(1), Article 2443666. https://doi.org/10.1080/10298436.2024.2443666

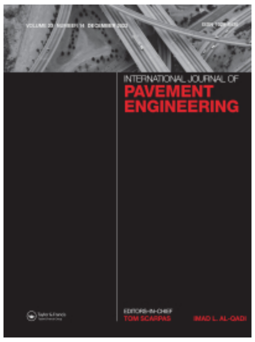

International Journal of Pavement Engineering

ISSN: (Print) (Online) Journal homepage: www.tandfonline.com/journals/gpav20

Investigations of thermal behaviours of asphalt pavement under short-term preheating technique for pavement overlay construction

Xinyi Song, Lijun Sun, Huailei Cheng, Hongchao Zhang, Zhanchuang Han, Yue Hu & Yi Li

To cite this article: Xinyi Song, Lijun Sun, Huailei Cheng, Hongchao Zhang, Zhanchuang Han, Yue Hu & Yi Li (2024) Investigations of thermal behaviours of asphalt pavement under short-term preheating technique for pavement overlay construction, International Journal of Pavement Engineering, 25:1, 2443666, DOI: 10.1080/10298436.2024.2443666

To link to this article: https://doi.org/10.1080/10298436.2024.2443666

Published online: 02 Jan 2025.

INTERNATIONAL JOURNAL OF PAVEMENT ENGINEERING
2024, VOL. 25, NO. 1, 2443666
https://doi.org/10.1080/10298436.2024.2443666

Taylor & Francis
Taylor & Francis Group

Investigations of thermal behaviours of asphalt pavement under short-term preheating technique for pavement overlay construction

Xinyi Song[a], Lijun Sun[a], Huailei Cheng[a,b], Hongchao Zhang[a], Zhanchuang Han[c], Yue Hu[a] and Yi Li[d]

[a]The Key Laboratory of Road and Traffic Engineering, Ministry of Education, Tongji University, Shanghai, People's Republic of China; [b]Shanxi Intelligent Transportation Laboratory Co., Ltd., Taiyuan, People's Republic of China; [c]National University of Singapore, Singapore; [d]Department of Engineering Structures, Faculty of Civil Engineering and Geosciences, Delft University of Technology, Delft, The Netherlands

ABSTRACT
Asphalt concrete overlay is typically designed to be thin to minimise maintenance and rehabilitation costs, which makes it challenging to be compacted and may affect its bonding conditions with the existing pavement. The short-term preheating involves swiftly heating the pavement surface before overlay paving commences, aiming to enhance the bonding conditions between the overlay and the existing pavement. Implementing the preheating approach requires a comprehensive understanding of thermal behaviours exhibited by existing pavement under short-term preheating and the factors affecting it. In this research, the feasibility of using electric heating tubes as short-term preheating heat source was analysed, and a finite element (FE) model for analysing the thermal behaviour of asphalt pavements under rapid preheating was developed. The key control parameter between the heat source and the pavement were determined and calibrated by field tests. Further sensitivity analyses of the effects of multiple factors on the thermal response of the pavement during rapid preheating were conducted, and a prediction model of the maximum pavement temperature achievable through preheating was developed. The established prediction model is expected to provide references for implementing short-term preheating in pavement overlay construction.

ARTICLE HISTORY
Received 1 July 2024
Accepted 12 December 2024

KEYWORDS
Asphalt pavement; Short-term preheating; Thermal responses; Thermal transfer coefficient; Field test

1. Introduction

Asphalt pavement undergoes typical distress over time due to repeated traffic loads and environmental impacts (Sun 2016, Cheng et al. 2021b, Cheng et al. 2022b, Yao et al. 2023). To restore the pavement's serviceability, regular maintenance or rehabilitation work is essential (Chen and Scullion 2015). Asphalt concrete overlay finds extensive use in pavement maintenance and rehabilitation, serving as an effective method to enhance performance and extend service life of the existing pavement (Koohmishi and Palassi 2015). During overlay construction, ensuring a strong bonding between the newly placed overlay layer and the existing pavement surface is crucial, as this bonding condition directly influences pavement distress such as cracking and debonding (Yang et al. 2012). However, overlay layers are typically designed to be thin to minimise maintenance and rehabilitation costs (Labi et al. 2005, Son et al. 2016). The reduced thickness makes the hot-mixed asphalt mixture vulnerable to rapid paving temperature decline, particularly on windy and cold days. This rapid decrease in paving temperature makes it challenging to compact the overlay layer to the required state (Liang 2022). Additionally, it hinders the formation of a satisfactory bonding between the asphalt mixture overlay and the existing pavement, increasing the risk of potential pavement distress after construction (Al-Hosainat et al. 2022). Therefore, it is imperative to focus on strategies to enhance bonding conditions, aiming to improve the in-service performance of pavement overlays (Sun 2016, Cheng et al. 2022b).

To enhance the service life of pavement overlays, this research introduces a new approach aimed at improving the bonding between the overlay and the existing pavement surface through preheating technology (Liu et al. 2020). The primary concept of this method involves swiftly preheating the existing pavement surface for a brief period before overlay paving commences (Chen and Wang 2024). This short-term preheating process rapidly elevates the temperature of the existing pavement within a certain depth, creating a hot supporting base for the overlay layer (Byzyka et al. 2022, Chen et al. 2023). This hot foundation serves a dual purpose: firstly, it helps maintain the temperature of the hot-mixed overlay materials during paving and aids in the compaction of the overlay layer (Qian et al. 2020). Secondly, the elevated temperature of the existing pavement surface holds significant potential for fostering better bonding with the overlay layer, transitioning the bonding condition between the two layers from the conventional 'cold pavement-hot overlay' mode to a more favourable 'hot pavement-hot overlay' mode (Apostolidis et al. 2020, Ghabchi and Dharmarathna, 2022).

The implementation of the preheating approach mentioned above in overlay construction requires a comprehensive understanding of the thermal behaviours exhibited by existing pavement under short-term preheating (Liu et al. 2019). These thermal behaviours serve as crucial references

CONTACT Huailei Cheng chl6218@tongji.edu.cn; Hongchao Zhang zhanghc@tongji.edu.cn

for designing preheating devices and optimising the construction process (Shamsaei et al. 2022). Existing research on the thermal behaviours of asphalt pavement primarily focuses on the field of hot in-place recycling (Gu et al. 2017). In hot in-place recycling, the old asphalt pavement must also be heated to restore the compacted asphalt mixture layer to a loose asphalt mixture (Makowska et al. 2017), which is then recycled and re-mixed with new aggregate and asphalt binder for paving. Various heating methods, such as the infrared method (Li et al. 2021), hot-air method (Xiao, 2022), microwave method (Sun and Sheng 2020, Maliszewski et al. 2021), and others, have been utilised by hot in-place recycling devices (XU et al. 2018). Researchers have explored the effects of multiple factors on the thermal behaviours of old pavement, including heating time, heater temperature, and heat source types (Du et al. 2013, Ma et al. 2020, Ma et al. 2022). These research findings aid in selecting an appropriate heating strategy for the hot in-place recycling of asphalt pavement (Ma et al. 2022). However, they provide limited guidance for the short-term preheating of asphalt pavement during overlay construction, primarily due to differences in heating duration(Byzyka et al. 2020). Hot in-place recycling necessitates that the temperature of the entire asphalt layer exceeds 100 °C, requiring a slow and prolonged heating process supported by a stable heating source from the devices (Li et al. 2016, Noojilla et al., 2022). In contrast, preheating old pavement during overlay is short-term and focuses on increasing pavement temperature near the surface (Chen et al. 2024). This brief heating period poses challenges, as the pavement temperature is easily influenced by environmental factors such as air temperature and wind. Moreover, short-term heating complicates the determination of thermal interaction behaviours between the asphalt pavement and heating source during analysis (Liu et al. 2024). Previous research assumes that these thermal interaction behaviours remain constant throughout the heating process (Ma et al. 2016, Li et al. 2023), which may hold true for the prolonged and stable heating process of hot in-place recycling (Alavi et al. 2014, Huang et al. 2016). However, for short-term preheating, these thermal interaction behaviours are unlikely to reach a stable state and thus require careful investigation to reflect actual conditions. In summary, the thermal behaviours of existing pavement under short-term preheating still require evaluation to facilitate the application of the preheating approach in overlay construction.

This research aims to investigate the thermal behaviours of asphalt pavement with short-term preheating for overlay construction. Firstly, the short-term preheating approach and the thermal transfer process from heating source to asphalt pavement were analysed. Secondly, the finite element (FE) model for analysing the thermal behaviours of asphalt pavement under preheating was established and subsequently calibrated via field tests. Finally, with the aid of the FE model, the impacts of multiple factors (e.g. heating temperature, initial pavement temperature, wind speed) on pavement's thermal responses during preheating were analysed. The prediction models for the maximum pavement temperature achievable through preheating were also developed. The organisation of the study is demonstrated in Figure 1. The findings in this research are expected to provide references for implementing short-term preheating in pavement overlay construction.

2. Short-term preheating approach and thermal transfer process

2.1. Short-term preheating approach

A short-term preheating approach is proposed to rapidly increase the temperature of the old pavement surface before paving and compacting the overlay materials. For illustrative purposes, Figure 2 depicts schematic diagrams of a preheating device and the corresponding preheating process. The preheating device consists of multiple parallel carbon fibre heating

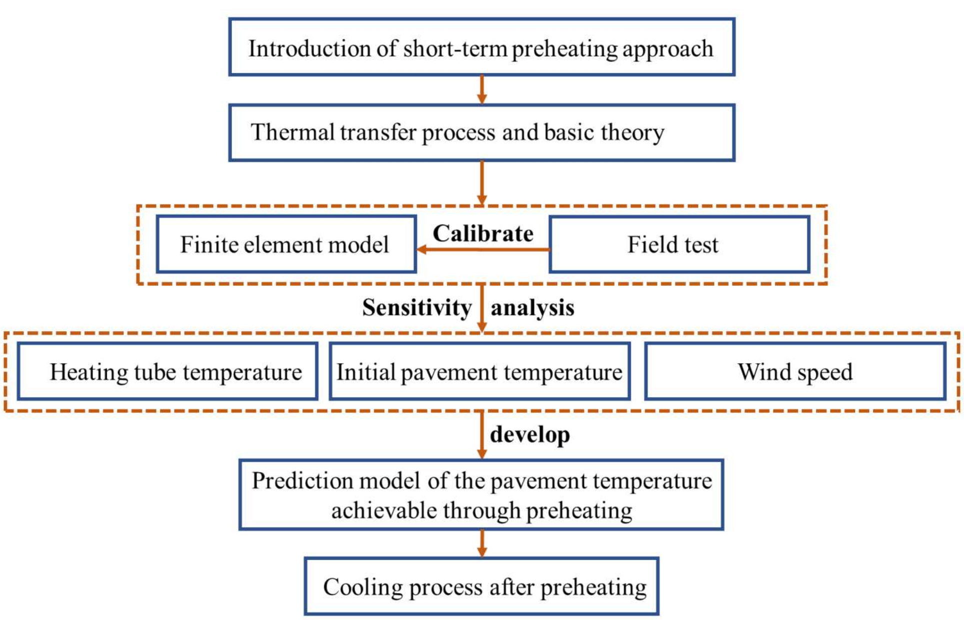

Figure 1. Flowchart of the research.

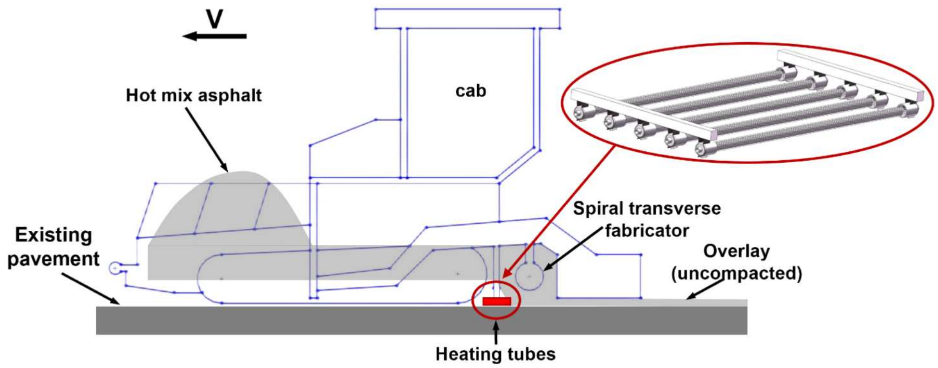

Figure 2. Short-term heating method and equipment.

tubes installed in front of the spiral feeder of the paver, positioned just above the existing pavement. As the paver moves, the heating tubes deliver heat to the pavement surface, rapidly raising its temperature. Following the preheating process, the hot mixed asphalt mixture for overlay construction is quickly paved and compacted onto the old pavement, establishing a robust 'hot pavement-hot overlay' bonding condition. The preheating device can also be mounted on rollers, bulldozers, and other construction equipment to accommodate various overlay construction projects and environmental conditions.

According to construction specifications, the paver's moving speed is typically controlled at 2~6 metres per minute for virgin asphalt mixture, with this speed reduced to 1~3 metres per minute for polymer-modified asphalt mixture. Consequently, the preheating duration for the pavement typically ranges from 10 to 60 s, depending on the paver's moving speed. A slower moving speed of the paver results in a longer heating duration on the existing pavement. This research focuses on investigating the thermal behaviours of the pavement during this short preheating duration. The findings from this investigation are expected to inform the design of the preheating device and the optimisation of overlay construction procedures under various environmental conditions.

2.2. Thermal transfer process

To assess the thermal behaviours of existing pavement during preheating, it's crucial to understand the detailed thermal transfer process from the heating source to the asphalt pavement. This study outlines the thermal interactions between the pavement and the heating source in Figure 3. It's observed that three thermal transfer modes exist during preheating: convection, conduction, and radiation. As the heating tubes approach the road surface, they warm up the air surrounding the pavement surface. The heated air then further transfers heat to the pavement surface, constituting a thermal transfer process known as convection. Meanwhile, a portion of the heat is directly transmitted to the pavement surface, leading to an increase in pavement temperature, which is defined as the thermal radiation mode. As the pavement surface gradually absorbs heat and warms up, it further transfers the heat to inside pavement, and this process is defined as conduction.

The following section will present the theoretical foundations of convection, conduction, and radiation modes involved in the thermal transfer process. This overview informs the development of a thermal model for analysing pavement temperature and forms the basis for the subsequent finite element modelling. Specifically, the thermal convection between the pavement and the heater, as mentioned earlier, can be quantified using Newton's cooling law, shown in Eq. (1) (Qian et al. 2020):

$$q = hT \tag{1}$$

Where, q is the heat flow density, h is convective thermal transfer coefficient between the heating source and

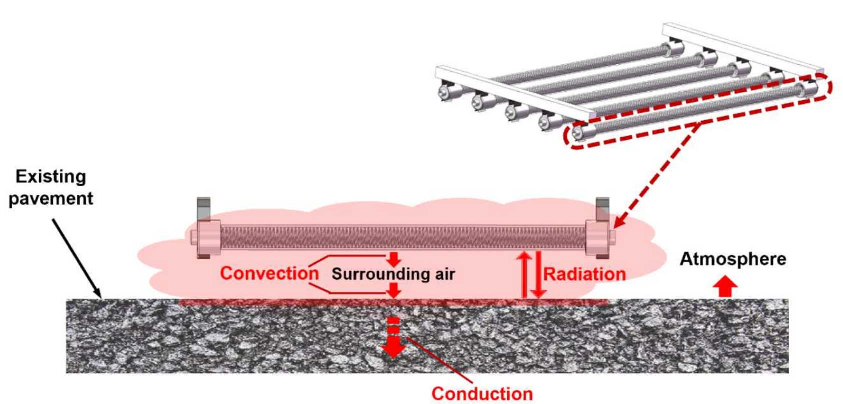

Figure 3. Thermal transfer modes during short-term heating process.

pavement, and T is the temperature difference heating source and pavement.

The convection process between the pavement surface and air can also be calculated using Eq. (1). However, the corresponding thermal transfer coefficient is affected by the wind speed (Qin, 2016), and it can be calculated using Eq. (2) (Zhao et al. 2020):

$$h_{wind} = 3.7v + 9.4 \tag{2}$$

Although convection occurs simultaneously on the pavement and between different objects, all of these processes adhere to the same physical laws, providing a theoretical basis for subsequent modelling and normalisation. Throughout this process, the thermal transfer coefficient (h) determines the efficiency of heat transfer, while the temperature difference (ΔT) acts as the driving force for the process, also influencing its overall efficiency.

For the thermal radiation process, the radiant heat emitted by an object above absolute zero per unit time and unit surface area can be computed using a modified version of the Stefan–Boltzmann law (Qian et al. 2020):

$$E = \varepsilon\sigma T^4 \tag{3}$$

Where, ε is the emissivity of the object, whose value is less than 1. σ is the Stefan-Boltz constant, i.e. 5.67×10^{-8}W/(m^2·K^4). T is the thermodynamic temperature of the object. Absolute zero is – 273.15 °C. The heat flow density q between any two points on different objects can be calculated as (Gong et al. 2023):

$$q = \frac{F\sigma}{\frac{1}{\varepsilon_A} + \frac{1}{\varepsilon_B} - 1}\left(T_A^4 - T_B^4\right) \tag{4}$$

Where, F is the radial angle coefficient, which depends on the relative position and distance between the objects. It is a function of the geometry or orientation of the two surfaces, taking values between 0 and 1. During the heating process, the temperature of the pavement surface is typically lower than that of the heating tube but higher than the surrounding air temperature. Consequently, the pavement surface absorbs radiation emitted by the heating tube and simultaneously converts its own thermal energy into radiant energy, which is then released to the surrounding air.

It is evident that radiation is not linearly related to the ΔT between objects. For further analysis, a heating condition is simulated using the commercial finite element software ABAQUS, where the relevant parameters for thermal radiation and convection are specified. The specific values of these parameters are not detailed here, as the focus is on analysing the relationship between different heat transfer modes. The modelling and simulation process will be described in detail in the subsequent sections. The magnitude of the pavement temperature increase induced by the two heat transfer effects under various heating durations is calculated using the finite element method, and the results are presented in Table 1.

The calculations reveal that during the short heating process (lasting less than 60 s), the ratio of pavement temperature increases due to convection and radiation remains relatively constant. This finding indicates that radiant heat transfer can be linearly converted into convective heat transfer, allowing for unified modelling in the subsequent phases of the analysis.

The thermal conduction from the pavement surface to the inside pavement can be analysed via a differential equation developed based on Fourier's law of thermal conductivity (Qian et al. 2020). According to the principle of conservation of energy, the thermal balance relationship between the micromeres at any time interval can be expressed as follows:

$$Q_{import} + Q_{generate} = Q_{export} + Q_{increment} \tag{5}$$

Where, Q_{import} is the total thermal imported into the micromeres, $Q_{generate}$ is the thermal generated by the heat source in the micromeres, Q_{export} is the total heat exported out of the micromeres, $Q_{increment}$ is the energy increments in the micromeres. By dividing the three-dimensional pavement into a finite number of microelement bodies, it is denoted that the thermal imported through the three microelement surfaces of any microelement body at $x = x_i$, $y = y_i$, and $z = z_i$ as Φ_x, Φ_y, and $\Phi_z$respectively. Similarly, the heat exported through the three microelement surfaces at $x = x_i + dx$, $y = y_i + dy$, and $z = z_i + dz$ as Φ_{x+dx}, Φ_{y+dy}, and Φ_{z+dz}. Here, λ is thermal conductivity which is a physical property of material, t is the pavement temperature field, τ denotes time, ρ and c are the density and specific heat capacity of the pavement. The above items are calculated by the following formulas:

$$\begin{cases} \Phi_x = -\lambda\left(\frac{\partial t}{\partial x}\right)dydz \\ \Phi_y = -\lambda\left(\frac{\partial t}{\partial y}\right)dxdz \\ \Phi_z = -\lambda\left(\frac{\partial t}{\partial z}\right)dxdy \end{cases} \tag{6}$$

Table 1. Temperature increases of pavement induced by different heat transfer effects.

Heating duration (s)	Radiation induced t_1 (°C)	Convection induced t_2 (°C)	$\frac{t_2}{t_1}$ (%)	$t_1 + t_2$ (°C)	Coexistence of the two effects t/°C	$\frac{t}{t_1 + t_2}$ (%)
10	52.2	63.6	1.218	115.8	92.9	80.2
20	65.4	79.9	1.222	145.3	119.6	82.3
30	75.1	91.3	1.216	166.4	138.2	83.1
40	83.1	100.4	1.208	183.5	152.8	83.3
50	90.0	108.1	1.201	198.1	164.8	83.2
60	96.0	114.6	1.194	210.6	175.1	83.1

$$\begin{cases} \Phi_{x+dx} = \Phi_x + \dfrac{\partial \Phi_x}{\partial x}dx = \Phi_x + \dfrac{\partial}{\partial x}\left[-\lambda\left(\dfrac{\partial t}{\partial x}\right)_x dydz\right]dx \\ \Phi_{y+dy} = \Phi_y + \dfrac{\partial \Phi_y}{\partial y}dy = \Phi_y + \dfrac{\partial}{\partial y}\left[-\lambda\left(\dfrac{\partial t}{\partial y}\right)_y dxdz\right]dy \\ \Phi_{z+dz} = \Phi_z + \dfrac{\partial \Phi_z}{\partial z}dz = \Phi_z + \dfrac{\partial}{\partial z}\left[-\lambda\left(\dfrac{\partial t}{\partial z}\right)_z dxdy\right]dz \end{cases} \quad (7)$$

As there is no thermal source within the microelement body of the pavement structure, the increment of internal energy in microelements is expressed as:

$$Q_{increment} = \frac{\rho ctdxdydz}{\tau} = \rho c\frac{\partial t}{\partial \tau}dxdydz \quad (8)$$

Substituting Eq. (6), (7), (8) into Eq. (5), the following differential equation for the thermal conductivity of the internal pavement can be derived:

$$\rho c\frac{\partial t}{\partial \tau} = \frac{\partial}{\partial x}\left(\lambda\frac{\partial t}{\partial x}\right) + \frac{\partial}{\partial y}\left(\lambda\frac{\partial t}{\partial y}\right) + \frac{\partial}{\partial z}\left(\lambda\frac{\partial t}{\partial z}\right) \quad (9)$$

For the purpose of exploring the feasibility and regularity of the technology, asphalt pavements with AC-13 mixture are taken for analysis and field experiments in this study. The thickness of the asphalt layer for the FE modelling of the pavement in this study is 4 cm due to the small depth range of the effect of short-term preheating on the pavement. This thickness enables to fulfil the adiabatic boundary conditions for FE model.

3. Thermal analysis model and parameters

3.1. 3D finite element modelling

Drawing on the theoretical framework of convection, conduction, and radiation modes in the thermal transfer process, this study develops a three-dimensional (3D) finite element (FE) model of asphalt pavement to analyse its thermal behaviours during preheating. The diagram of the developed FE model is presented in Figure 4(a). In the FE model, the carbon fibre heating tube is cylindrical, with a radius of 0.5 cm and a height of 30 cm, settled 2 mm above the pavement surface. The asphalt pavement's dimensions in the FE model are 4 m in length, 4 m in width, and 0.4 m in depth. A fine mesh is applied near the model centre, while a relatively coarse mesh is utilised for areas farther from the centre. The mesh size near the model centre is assigned as 1 cm × 1 cm × 0.1 cm, which has been approved to meet the convergence requirement (Cheng et al. 2021a, Cheng et al. 2021c, Cheng et al. 2022a). The total model is divided into 576,000 elements. The thermal DC3D8 element is used to build a model for thermal analysis. The FE model allows for the adjustment of multiple preheating scenarios, including heating device temperature, air temperature, initial pavement surface temperature, and heating duration, to elucidate the impacts of preheating conditions on the thermal behaviours of asphalt pavement. Exemplary calculation results of pavement surface temperature from the FE model are presented in Figure 4(b).

3.2. Determination of key thermal parameters in the FE model

Based on the previous analysis, it is established that the heating effects of different heat transfer modes on the pavement can be linearly transformed and unified during the short-term heating process. Therefore, this study adopts the thermal transfer coefficient of convection as the key control parameter for describing the entire heating process. It is posited that this coefficient is influenced by the initial temperature state of each object. The measured thermal transfer coefficient, obtained through calibration of the experimental data, reflects the average behaviour of the entire short-term heating process.

The necessary model parameters are summarised in Table 2. Notably, some model parameters can be directly determined based on the preheating device and environmental conditions. These include the heating tube temperature, initial road surface temperature, air temperature, wind speed, and heating duration, all of which are explicitly specified in the 'Load,' 'Interaction,' and 'Step' modules of the software. Additionally, thermal parameters related to the radiation process, such as the emissivity coefficient and radial angle coefficient, as well as those pertaining to the conduction process, including density, heat capacity, and thermal conductivity, can be appropriately defined based on the physical properties of the heating device and asphalt mixture. These parameters are inputted into the 'Property' and 'Interaction' modules. In contrast, the thermal transfer coefficient between the pavement and the heating device is influenced by multiple factors and requires careful determination to accurately represent the actual thermal behaviours of asphalt pavement during preheating. The thermal interaction between the pavement and the heating device is established in the 'Interaction' module, where the type is set to 'Surface-to-surface contact (Standard),' allowing the thermal transfer coefficient to be adjusted for simulating various preheating scenarios.

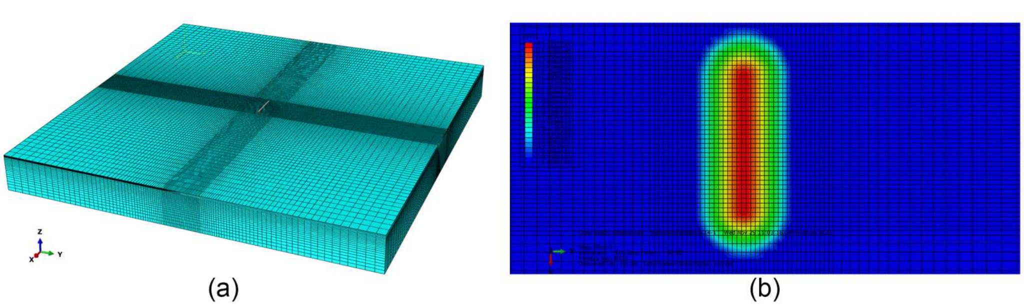

Figure 4. The diagrams of (a) the developed FE model and (b) the model calculation results.

Table 2. Parameters settled in the FE model.

Parameter	Unit	Value
Heating tube temperature	°C	Determined according to tube settlements
Initial pavement surface temperature	°C	Determined according to field conditions
air temperature	°C	Determined according to field conditions
Thermal transfer coefficient	$W/(m^2{\cdot}K)$	Needs to be calibrated
Emissivity coefficient of heating tubes	/	0.92
Emissivity coefficient of pavement surfaces	/	0.9
Radial angle coefficient	/	1
Wind speed	m/s	Determined according to field conditions
Heating duration	s	Determined according to preheating settlements
Thermal conductivity of pavement	W/(m·K)	1.3
Specific heat of pavement	J/(kg·°C)	924.9
Density of pavement	kg/m^3	2300

In this study, field pavement temperature measurements during in-situ preheating tests were utilised to calibrate the FE model and derive the thermal transfer coefficient. The detailed calibration process will be introduced in the next section.

4. Calibration of FE model

4.1. Field preheating test and temperature measurements

To calibrate the FE model, field preheating tests were conducted on the in-situ asphalt pavement to measure its actual thermal behaviours. The preheating device used in the test was a carbon fibre heating tube, encased in a high-temperature quartz glass outer layer to protect the carbon fibre. The dimensions of the heating tube matched those settled in the FE model, with a radius of 0.5 cm and a height of 30 cm. Throughout preheating, the tube was positioned 2 mm above the asphalt pavement. The configuration of the heating tube is illustrated in Figure 5(a).

An electronic thyristor regulator was employed to adjust the input voltage of the heating tube, thereby controlling its output temperature. The output temperature of the tube was varied between 400°C and 550°C to examine its effects on the thermal behaviours of the existing asphalt pavement. The schematic of the thyristor electronic regulator is depicted in Figure 5(b).

Two heating durations, namely 30s and 60s, were tested in the field. During the heating test, an infrared thermal imaging camera was utilised to measure the temperature at the asphalt pavement's surface, as illustrated in Figure 5(c). This camera facilitated the acquisition of a cloud map showing the temperature distribution across the pavement surface.

Regarding environmental and pavement conditions in field tests, the initial temperature at the pavement surface was approximately 20°C, with a wind speed of roughly 1 m/s. The temperature field on the pavement surface during the preheating process was recorded using the infrared thermal imaging camera. Figure 6 presents an exemplary cloud map illustrating the distribution of pavement temperatures.

Using the recorded temperature cloud maps, the maximum temperatures at the pavement surface after preheating were determined and analysed. The changing trends of the maximum pavement temperatures with the heating tube temperatures and heating durations are depicted in Figure 7. It is evident that the maximum pavement temperature increases with the rise in the heating tube temperature, as expected, due to increased thermal transfer to the pavement. Similarly, when the heating tube temperature remains constant, the maximum pavement temperature increases with longer heating durations, as this allows for more thermal interactions between the heating tube and the pavement.

4.2. Model calibration

The pavement temperature data obtained from the field preheating test were utilised to calibrate the FE model, ensuring its reliability. As outlined in Section 3.2, the thermal transfer coefficient within the FE model emerged as a crucial parameter requiring precise calibration. Consequently, this study computed pavement temperatures using varying levels of thermal transfer coefficients as input, and subsequently compared these calculated temperatures with the field-measured ones. Figure 8 illustrates the comparisons between the calculated and field-measured temperatures, with a noteworthy point being that the heating duration for the data in Figure 8 is 30s.

Figure 8 clearly demonstrates the challenge of using a constant thermal transfer coefficient to simulate the thermal behaviours of asphalt pavement under different levels of heating tube temperature. Conversely, adjusting the thermal transfer coefficient in tandem with the changing tube temperature is

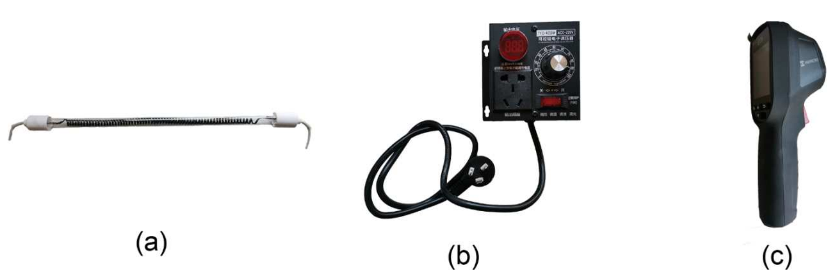

Figure 5. Test apparatus and equipment: (a) Carbon Fiber Heating Tube; (b) Thyristor electronic regulator; (c) Infrared Thermal Imaging Camera.

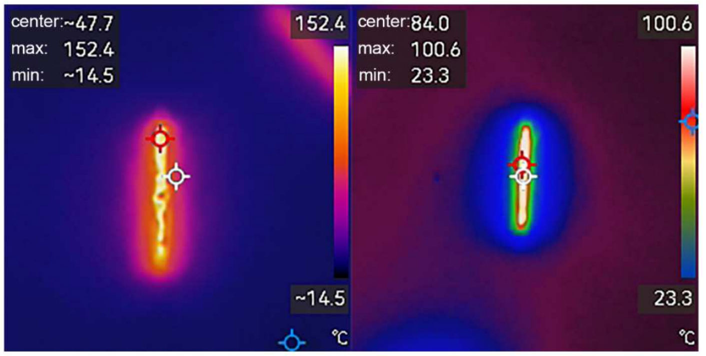

Figure 6. Cloud map of pavement temperature distribution recorded by thermal imaging camera.

necessary to generate satisfactory pavement temperature predictions. This observation underscores the influence of tube temperature on the thermal interactions between the heating tube and the pavement. Consequently, determining appropriate thermal transfer coefficients in the FE model becomes essential for accurately reflecting the thermal impacts of heating tubes with various temperatures.

Utilising the data from Figure 8, the thermal transfer coefficients corresponding to different tube temperatures were calculated using the interpolation method. The calculation results are summarised in Table 3. It is evident that the thermal transfer coefficient increases as the tube temperature rises, indicating a stronger thermal interaction between the tube and the pavement with increasing tube temperature. Relationships between the thermal transfer coefficients and the tube temperatures were also established in this study, as depicted in Figure 9. It is observed that the thermal transfer coefficients increase with the rise of tube temperatures, following an approximately exponential function trend. The fitted correlation coefficient reaches 0.912, indicating a strong correlation between the thermal transfer coefficient and the tube temperature. Based on the exponential function illustrated in Figure 9, it is convenient to determine the appropriate thermal transfer coefficient in FE model to analyse the thermal behaviours of asphalt pavement under preheating.

The thermal transfer coefficients depicted in Figure 9 were derived from field pavement temperature measurements associated with a preheating duration of 30s. However, as mentioned, pavement temperatures with a preheating duration of 60s were also measured in the field test. Consequently, temperature measurements corresponding to a preheating duration of 60s were utilised further to validate the accuracy of these thermal transfer coefficients. Specifically, the thermal transfer coefficients were applied in the FE model to predict pavement temperatures after 60s of preheating. The predicted temperatures were then compared with the field-measured ones, and the comparison results are presented in Figure 10.

Evidently, the calculated pavement temperatures closely align with the field-measured pavement temperatures, regardless of the heating tube temperatures. The average deviation between the calculated and field-measured temperatures is only 5.72%, confirming that the FE model is capable of generating accurate simulations of pavement temperatures after preheating. These simulation results also demonstrate that the applied thermal transfer coefficients effectively reflect the thermal interactions between the heating tube and the pavement. With these thermal transfer coefficients as input, the thermal behaviours of asphalt pavement under other preheating scenarios can be determined using the FE model.

5. Preheating temperature model sensitive analysis

Utilising the FE model and the calibrated thermal transfer coefficients, the thermal behaviours of asphalt pavement under a wide range of preheating scenarios were calculated. These scenarios encompass different combinations of heating tube temperatures, initial pavement surface temperatures, and wind speeds. The computed results provide crucial references for analysing the

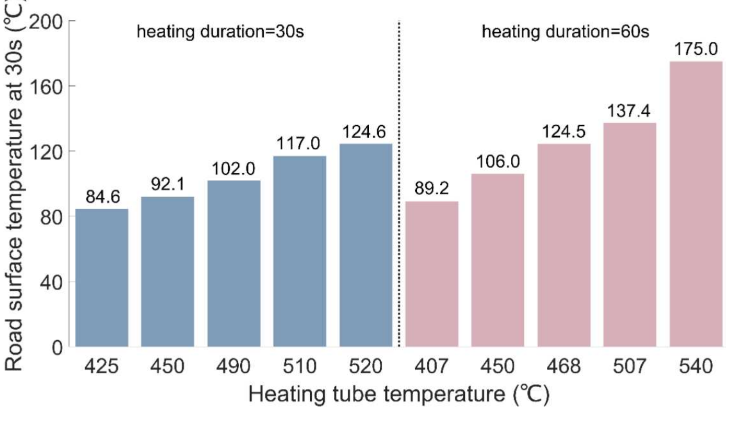

Figure 7. Field pavement heating test results.

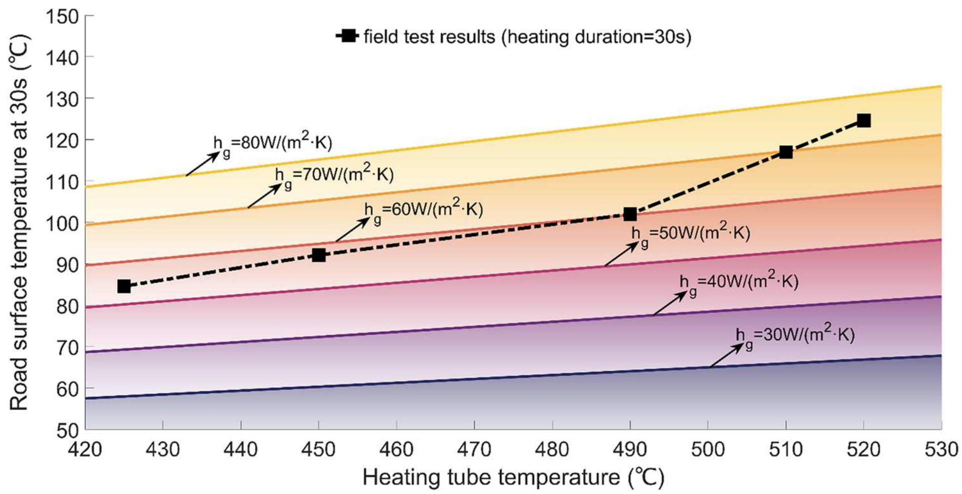

Figure 8. Comparisons between the calculated and the field-measured temperatures.

Table 3. Thermal transfer coefficients for different heating tube temperatures.

Heating tube temperature T_{heater_j} (°C)	Maximum temperature of measured road surface $T_{surface\_max\_j}$ (°C)	Thermal transfer coefficient h_{g_j} (W/(m²·K))
425	84.6	56.06
450	92.1	59.32
490	102.0	62.03
510	117.0	71.41
520	124.6	75.91

impacts of multiple factors on pavement temperatures during preheating, thereby guiding the optimisation of the preheating procedure to achieve desirable pavement heating states.

5.1. Impacts of heating tube temperatures

Five magnitudes of heating tube temperatures, namely 300°C, 400°C, 500°C, 600°C, and 700°C, were considered in this study. Using these heating tube temperatures as input, the maximum pavement temperatures during 30s of heating were simulated and compared in Figure 11. It is noteworthy that the initial pavement temperature remains at 20°C, and the wind speed is maintained at 2 m/s.

It is observed that the pavement temperature gradually increases with the duration of heating. During the initial stage of preheating (i.e. < 5s), the pavement temperature experiences a rapid ascent with increasing heating duration. However, after this initial stage, the pavement temperature rises much more gradually, exhibiting a roughly linear relationship with the duration, suggesting that the thermal interactions between the heating tube and the pavement reach a stable state. Furthermore, the heating tube temperatures notably influence the maximum pavement temperature. As the heating tube temperature increases, the maximum pavement temperature rises accordingly. This observation indicates that increasing the tube temperature constitutes an effective means of elevating the pavement surface temperature.

5.2. Impacts of initial pavement temperature

The impacts of initial pavement temperatures on the maximum pavement temperature after preheating were also assessed. Six levels of initial pavement temperatures were included for analysis: – 10°C, 0°C, 10°C, 20°C, 30°C, and 40°

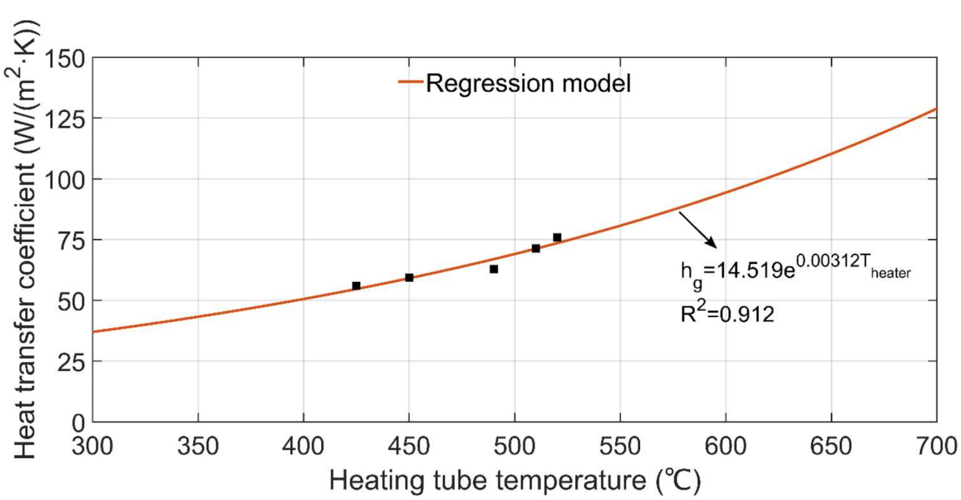

Figure 9. Thermal transfer coefficients at different tube temperatures.

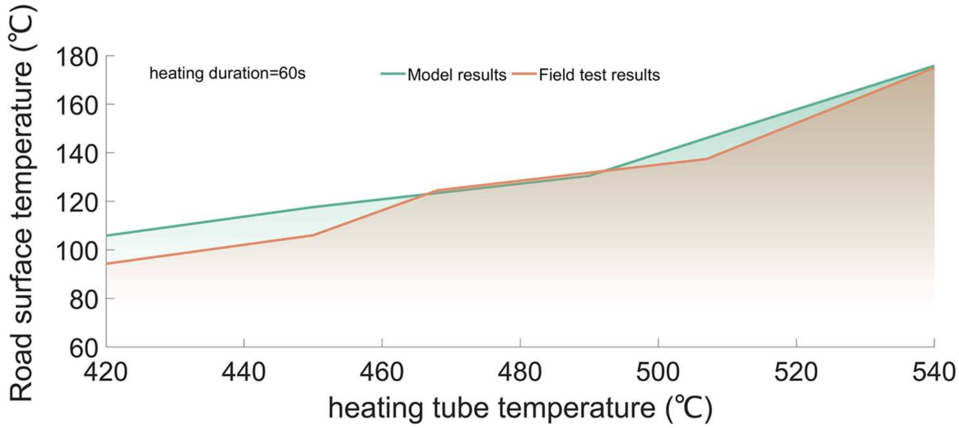

Figure 10. Comparison of calculated and field-measured pavement temperatures after 60s preheating.

C. Using these initial pavement temperature values as input, the pavement temperatures during 30s of preheating were calculated and presented in Figure 12. It is important to note that the heating tube temperature was maintained at a constant 500°C, while the wind speed remained constant at 2 m/s.

As illustrated in Figure 12, the pavement temperature demonstrates similar varying trends with the increase in heating duration, regardless of the initial pavement temperatures. Specifically, the pavement temperature experiences a rapid ascent during the initial preheating stage, followed by a smoother increase as the preheating continues. The initial pavement temperature noticeably influences its maximum temperature after 30s of preheating. As the initial pavement temperature increases, the maximum pavement temperature rises roughly linearly. This phenomenon suggests that conducting the preheating work in warm or hot weather conditions contributes to further elevating the pavement surface temperature.

5.3. Impacts of wind speed

The impacts of wind speeds on the maximum pavement temperature are depicted in Figure 13. Five levels of wind speeds were considered in this study: 0, 2, 4, 6, and 8 m/s, respectively. During calculation, the initial pavement temperature was maintained at 20°C, while the heating tube temperature was held constant at 500°C. Figure 13 suggests that the effects of wind speed on pavement temperatures are less pronounced compared to other factors, such as heating tube temperature and initial pavement temperature.

As the wind speed increases, the maximum pavement temperatures experience a mild decline. This is primarily due to the wind cooling the air near the pavement surface, thereby reducing the pavement temperature. Results in Figure 13 also demonstrate that windy weather has minimal impacts on pavement temperatures after preheating. Consequently, heating the pavement surface to the required temperature remains feasible even under strong wind conditions at the field site.

5.4. Prediction model for the maximum pavement temperature

Based on the findings presented in Sections 5.1–5.3, the multi-factor analysis of variance (ANOVA) was conducted to evaluate the significance level (*P*-value) of different influencing factors, with the results summarised in Table 4. The significance level (α) of ANOVAL analysis was set to 0.05 as usual. It is seen that the temperature of the heating tube has the most substantial impact on the pavement temperature, with an F-value of 13,738.90. The initial pavement temperature factor yields an F-value of 251.35, indicating that variations in the initial

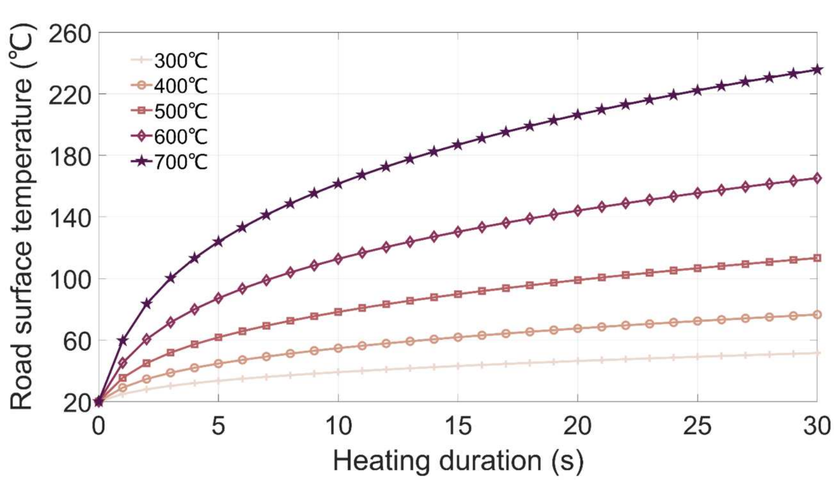

Figure 11. The maximum pavement temperatures under different heating tube temperatures.

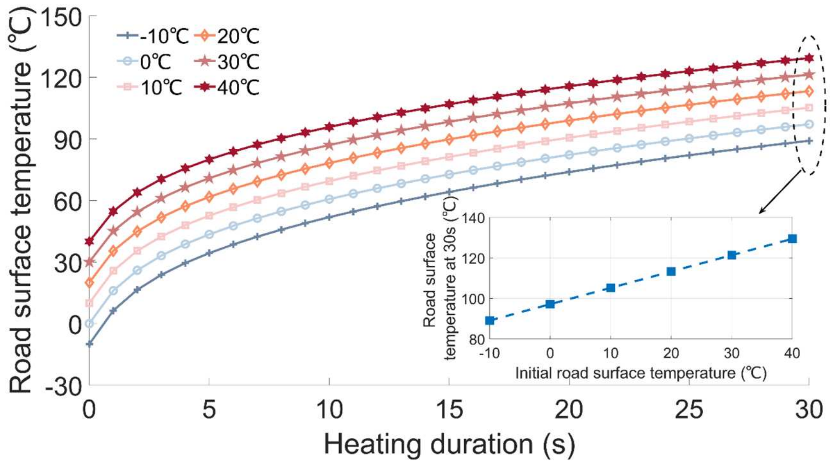

Figure 12. The maximum pavement temperatures under different wind speeds.

pavement temperature also significantly affect the final achievable temperature. In comparison, the wind speed generates a F-value of 20.40, demonstrating a comparatively slighter influence on the pavement heating process.

Figure 14 vividly illustrates the fluctuating trends of the maximum pavement temperatures following preheating with different heating tube temperatures and initial pavement temperatures. It is evident that the heating tube temperature exerts the most significant influence on the maximum pavement temperature, followed by the initial pavement temperature. Additionally, it is noteworthy that wind speed also impacts the maximum pavement temperature, albeit to a lesser extent compared to the tube temperature and initial pavement temperature. Consequently, the varying trend of the maximum pavement temperatures with the wind speed is not depicted in Figure 14. Building upon the insights gained from Figure 14, a predictive model was formulated to estimate the maximum pavement temperature during preheating, as represented by Equation (10).

$$T_{surface} = k_i \cdot T_{initial} + (k_w \cdot v_{wind} + k_h \cdot T_{heater}) \cdot \ln(d) + k_0 \tag{10}$$

Where, $T_{surface}$ is the maximum pavement surface temperature after preheating (°C), $T_{initial}$,v_{wind}, T_{heater},d are the initial pavement surface temperature(°C), the wind speed(m/s), the heating tube temperature(°C) and the preheating duration(s), respectively, and k_i, k_w, k_h, k_0 are the regression coefficients of the corresponding factors.

It is essential to note that the maximum pavement temperature is correlated with the duration of preheating. A prolonged preheating duration leads to a higher pavement temperature. In the development of predictive models, six distinct preheating durations were examined: 10, 20, 30, 40, 50 and 60 s. The resulting predictive model for the maximum pavement temperature following different preheating durations is delineated

Table 4. Results of analysis of variance.

Factor	Sum square	Degrees of freedom	Mean square	F	*P*
Heating tube temperature (°C)	222714.52	4	55678.63	13738.90	−0.001
Initial pavement temperature (°C)	5093.09	5	1018.62	251.35	
Wind speed (°C)	330.67	4	82.67	20.40	

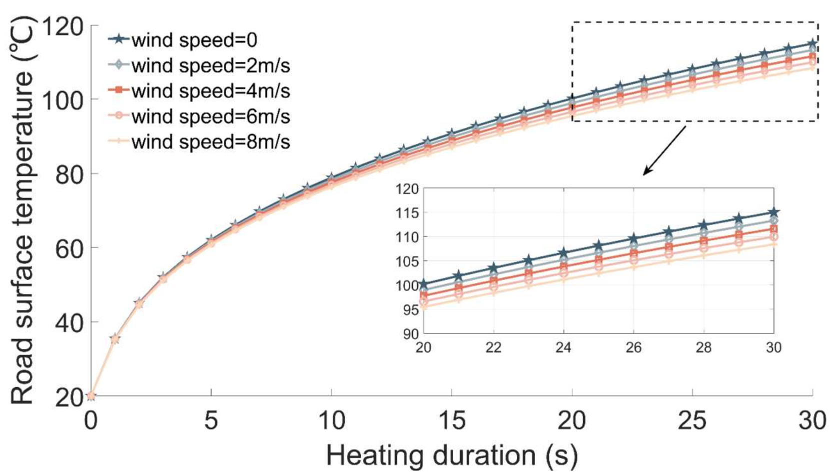

Figure 13. Temperature increase process of pavement in different wind speed environments within 30s of heating.

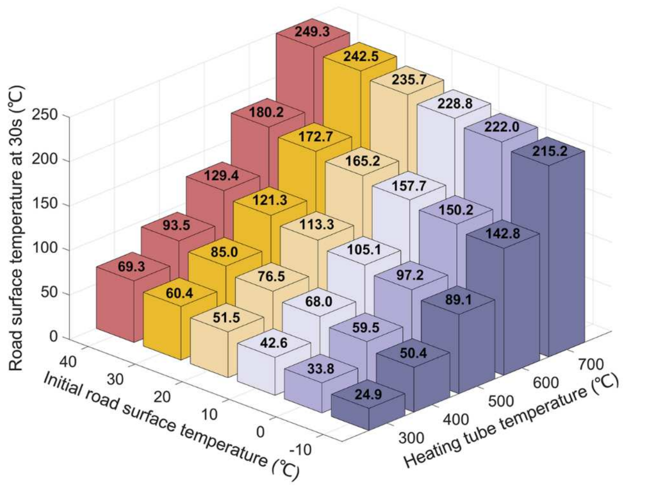

Figure 14. Road surface temperature after 30-second heating under different conditions.

in Equation (11). Notably, the correlation coefficient of the fitting model is 0.933, indicating the validity of the developed models in predicting the thermal behaviour of asphalt pavement with preheating. The model is anticipated to serve as crucial references for estimating pavement temperature during the preheating process, thereby facilitating the organisation of preheating activities to achieve the desired pavement temperature.

$$T_{surface} = 0.797 \cdot T_{initial} + (-0.785 \cdot v_{wind} + 0.121 \cdot T_{heater}) \cdot \ln(d) - 88.671 \quad (11)$$

6. Analysis of cooling process of pavement

In the aforementioned sections, the thermal behaviour of asphalt pavement during the preheating process was comprehensively evaluated and analysed. Subsequent to the removal of the preheating device, the asphalt pavement undergoes a cooling process. This study delves further into investigating the cooling process of the asphalt pavement following the cessation of preheating. The anticipated results of this investigation aim to quantify the temperature variation trend of the pavement during the cooling process and furnish indispensable references for organising subsequent pavement overlay construction.

The cooling process of the asphalt pavement was also simulated using an FE model, with the typical temperature variation trends of the asphalt pavement with cooling time illustrated in Figure 15. Additionally, detailed pavement temperatures after various cooling durations are summarised in Table 5. For this simulation case, the heating tube temperature utilised for preheating was set at 520°C, with a preheating duration of 60 s. The initial pavement temperature was 20°C, and the wind speed was maintained at 1 m/s. The cooling time was set to 5 minutes.

As depicted in Figure 15, the pavement temperature undergoes a rapid decline upon the removal of the preheating device, particularly noticeable near the pavement surface. Specifically, the pavement surface temperature decreases from 157.8°C to 120.1°C after only 4 s of cooling, further dropping to below 100°C after approximately 10 s of cooling. This observation underscores the necessity of commencing pavement overlay construction immediately after the preheating procedure concludes, ensuring that the existing pavement retains its high-temperature state. Conversely, the temperature at the bottom of the pavement experiences a more gradual decline, with roughly a 10°C decrease after 32 s of cooling. The findings of this investigation illustrate the advantages of the preheating approach proposed in section 2.1, which is able to significantly reduce heat losses and hence reducing energy usage.

7. Conclusions and Recommendations

This research aims to investigate the thermal behaviours of asphalt pavement with short-term preheating via finite element (FE) model and the calibrated thermal parameters. The main conclusions are summarised as follows:

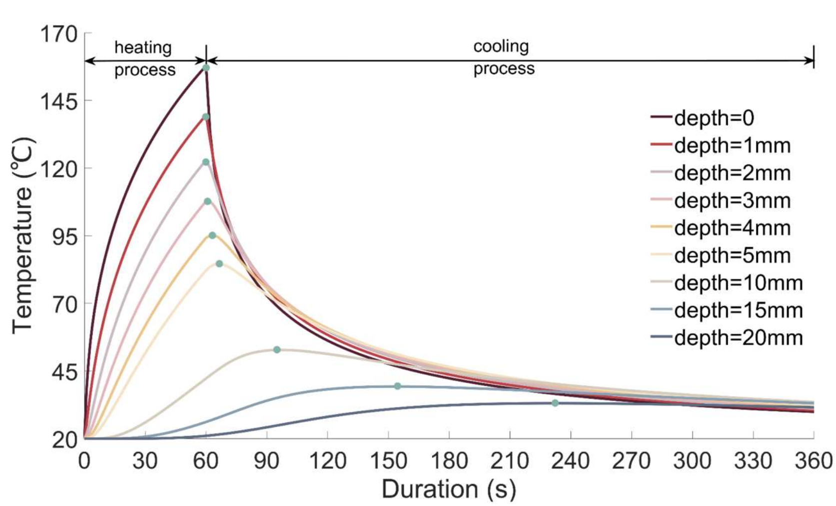

Figure 15. Temperature variations at different depths within the pavement structure during the cooling process.

Table 5. Cooling process of asphalt pavement at different depths.

Depth (mm)	0	1	2	3	4	5
Temperature just after preheating (°C)	157.8	139.6	122.9	107.8	94.2	82.2
Temperature after 4s cooling (°C)	120.1	121.5	115.6	106.0	95.2	84.4
Temperature after 8s cooling (°C)	105.2	108.3	106.4	100.9	93.2	84.4
Temperature after 12s cooling (°C)	95.7	98.9	98.7	95.4	89.9	83.1
Temperature after 16s cooling (°C)	88.6	91.8	92.3	90.4	86.4	81.1
Temperature after 20s cooling (°C)	83.0	86.1	87.1	85.9	83.1	78.8
Temperature after 24s cooling (°C)	78.4	81.4	82.6	82.0	79.9	76.5
Temperature after 28s cooling (°C)	74.5	77.4	78.8	78.6	77.0	77.3
Temperature after 32s cooling (°C)	71.2	74.0	75.4	75.5	74.3	72.1

(1) Calibrations on FE model reveal that the thermal transfer coefficient increases as the tube temperature rises, indicating a stronger thermal interaction between the tube and the pavement with increasing tube temperature. Relationships between the thermal transfer coefficients and the tube temperatures were established in this research, to guide determining the appropriate thermal transfer coefficient in FE model for pavement temperature analysis.
(2) The heating tube temperatures and the initial pavement temperature notably influence the thermal behaviours of asphalt pavement under short-term preheating. As the heating tube temperature or the initial pavement temperature increases, the maximum pavement temperature after preheating rises accordingly. By contrast, the wind speed shows a less apparent impacts on the thermal responses of asphalt pavement.
(3) The prediction models for the maximum pavement temperature resulting from preheating were developed. The correlation coefficient for the prediction model is 0.933, indicating the validity of the developed models in predicting the thermal behaviour of asphalt pavement. The model is anticipated to serve as a crucial reference for estimating pavement temperature during the preheating process, thereby facilitating the organisation of preheating activities to achieve the desired pavement temperature.
(4) Analysis of the cooling process after preheating indicates that the pavement temperature undergoes a rapid decline upon the removal of the preheating device, particularly noticeable near the pavement surface. Specifically, the pavement surface temperature decreases from 157.8°C to 120.1°C after only 4 s of cooling, further dropping to below 100°C after approximately 10 s of cooling. This observation underscores the necessity of commencing pavement overlay construction immediately after the preheating procedure concludes, ensuring that the existing pavement retains its high-temperature state.

It is important to mention the limitations of this study. First, only the heating effect of a single carbon fibre heating tube on asphalt pavement was examined. Additionally, the pavement material and structure evaluated in this research is limited. Future research is required to cover a broader range of asphalt pavement materials and structures to result in more general conclusions. These future efforts will be essential to further reveal the thermal mechanism of asphalt pavement under preheating and optimise the application of this technology in pavement overlay construction.

Acknowledgements

The research was supported by the National Key R&D Program of China (grant number: 2023YFA1008904) and the open project special fund of Intelligent Transportation Laboratory in Shanxi Province (grant number: 2024-ITLOP-TJ-02). The sponsorships are greatly appreciated.

Disclosure statement

No potential conflict of interest was reported by the authors.

Funding

This work was supported by National Key Research and Development Program of China: [Grant Number 2023YFA1008904]; open project special fund of Intelligent Transportation Laboratory in Shanxi Province: [Grant Number 2024-ITLOP-TJ-02]; Key Engineering Science and Technology Project of Jiangxi Provincial Department of Transportation: [Grant Number 2024ZG006].

References

Al-Hosainat, A., *et al.*, 2022. A comprehensive laboratory evaluation of the factors affecting the micro-surfacing interlayer bond strength. *Construction and Building Materials*, 323.

Alavi, M.Z., Pouranian, M.R., and Hajj, E.Y., 2014. Prediction of asphalt pavement temperature profile with finite control volume method. *Transportation Research Record*, 2456, 96–106.

Apostolidis, P., *et al.*, 2020. Use of epoxy asphalt as surfacing and tack coat material for roadway pavements. *Construction and Building Materials*, 250.

Byzyka, J., *et al.*, 2022. Performance enhancement of asphalt patch repair with innovative heating strategy. *Proceedings of the Institution of Civil Engineers-Transport*, 175, 300–309.

Byzyka, J., Rahman, M., and Chamberlain, D.A., 2020. Thermal analysis of hot mix asphalt pothole repair by finite-element method. *Journal of Transportation Engineering Part B-Pavements*, 146, 11.

Chen, J.Q., *et al.*, 2024. Modeling and analysis of ice condensation on bridge deck pavement surface based on heat transfer theory and finite element method. *Applied Thermal Engineering*, 241, 18.

Chen, D., and Scullion, T., 2015. Very thin overlays in Texas. *Construction & Building Materials*, 95, 108–116.

Chen, X., and Wang, H., 2024. Asphalt pavement pothole repair with recycled material and preheating: laboratory and field evaluation. *Journal of Cleaner Production*, 434, 11.

Chen, X., Wang, H., and Venkiteela, G., 2023. Asphalt pavement pothole repair using the pre-heating method: An integrated experiment and modeling study. *Transportation Research Record*, 2677, 1–12.

Cheng, H., *et al.*, 2021b. Effects of using different dynamic moduli on predicted asphalt pavement responses in mechanistic pavement design. *Road Materials and Pavement Design*, 23, 1860–1876.

Cheng, H.L., *et al.*, 2021c. Critical position of fatigue damage within asphalt pavement considering temperature and strain distribution. *International Journal of Pavement Engineering*, 22, 1773–1784.

Cheng, H., *et al.*, 2022b. Analysis of fatigue behaviors of asphalt mixture under actual loading waveforms using pseudo-strain-based approaches. *International Journal of Pavement Engineering*, 24, 1–14.

Cheng, H., Liu, L., and Sun, L., 2021a. Critical response analysis of steel deck pavement based on viscoelastic finite element model. *International Journal of Pavement Engineering*, 22, 307–318.

Cheng, H., Liu, L., and Sun, L., 2022a. Bridging the gap between laboratory and field moduli of asphalt layer for pavement design and assessment: A comprehensive loading frequency-based approach. *Frontiers of Structural and Civil Engineering*, 16, 267–280.

Du, L., Li, Y., and Li, C., 2013. Analyse the influence factors of energy-saving and emission-reduction in asphalt pavement construction. International Forum on Mechanical and Material Engineering (IFMME 2013), Jun 13-14 2013 Guangzhou, PEOPLES R CHINA. 913-918.

Ghabchi, R., and Dharmarathna, C.P., 2022. Effect of tack coat emulsion type, application rate, and surface type and texture on early-age interlayer shear strength of pavements in cold regions. *International Journal of Pavement Engineering*, 23, 1881–1896.

Gong, M., Sun, Y., and Chen, J., 2023. Numerical investigation on coupled thermo-mechanical critical response of curved ramp bridge deck pavement. *Road Materials and Pavement Design*, 24, 2048–2068.

Gu, H., *et al.*, 2017. Asphalt pavement heating speed in multi-stage hot in-place recycling. *China Journal of Highway and Transport*, 30, 170–176.

Huang, K., *et al.*, 2016. The feasibility of DEM to analyze the temperature field of asphalt mixture. *Construction and Building Materials*, 106, 592–599.

Koohmishi, M., and Palassi, M., 2015. Evaluation of application of thin HMA overlay on the existing flexible pavement for high-traffic-volume rural highways(article). *Periodica Polytechnica Civil Engineering*, 59, 65–75.

Labi, S., *et al.*, 2005. Analysis of long-term effectiveness of thin hot-mix asphaltic concrete overlay treatments. *Transportation Research Record*, 1940, 2–12.

Li, X., *et al.*, 2021. Numerical simulation analysis on heating effects of asphalt pavement by infrared and hot air compounding heating. *Journal of Southeast University. Natural Science Edition*, 51, 658–663.

Li, Z., *et al.*, 2023. Simulation analysis and optimization of temperature field for hot in-place asphalt pavement recycling. *Journal of Transportation Engineering, Part B: Pavements*, 149, 1–10.

Li, X., Ma, D., and Yang, S., 2016. Heating method for in-place heat recycling of asphalt pavement. *Journal of Central South University (Science and Technology)*, 47, 1290–1296.

Liang, Y., 2022. *Research on Heat Dissipation Characteristics and Construction Control of Thin Overlay of Asphalt Mixture.* Master's Thesis, Chongqing Jiaotong University.

Liu, Y., *et al.*, 2019. Effects of preheating conditions on performance and workability of hot in-place recycled asphalt mixtures. *Construction and Building Materials*, 226, 288–298.

Liu, Y., *et al.*, 2020. Study on impact of variables to pavement preheating operation in HIR by using FEM. *Construction and Building Materials*, 243, 11.

Liu, P.S., Rui, D.W., and Wang, S.Y., 2024. Structure and mechanism of directional heat induced asphalt pavement with thermal aggregation effect. *Construction and Building Materials*, 431, 11.

Ma, D., *et al.*, 2016. Design of asphalt mixture stirring roller and simulation and validation of heating efficiency. *Transactions of the Chinese Society of Agricultural Engineering*, 32, 104–109.

Ma, D., Chen, C., and Gui, X., 2022. Analysis of infrared radiation heating wavelength range of asphalt pavement. *Journal of Southeast University. Natural Science Edition*, 52, 730–735.

Ma, D., Yao, J., and Cao, Y., 2020. Influence of heating distance and wind speed on coupling heating asphalt pavement. *Journal of Huazhong University of Science and Technology. Nature Science*, 48, 67–72.

Makowska, M., Aromaa, K., and Pellinen, T., 2017. The rheological transformation of bitumen during the recycling of repetitively aged asphalt pavement. *Road Materials and Pavement Design*, 18, 50–65.

Maliszewski, M., *et al.*, 2021. Full-scale use of microwave heating in construction of longitudinal joints and crack healing in asphalt pavements. *Materials*, 14.

Noojilla, S.L.A., Kusam, S.R., and IEEE. 2022. Finite Element Modeling of Microwave applicator for heating Asphalt pavements. Asia-Pacific Microwave Conference (APMC), Nov 29-Dec 02 2022 Yokohama, JAPAN. 925-927.

Qian, G., *et al.*, 2020. Research on the affecting factors and characteristic of asphalt mixture temperature field during compaction. *Construction & Building Materials*, 257, 119509.

Qin, Y., 2016. Pavement surface maximum temperature increases linearly with solar absorption and reciprocal thermal inertial. *International Journal of Heat and Mass Transfer*, 97, 391–399.

Shamsaei, M., Carter, A., and Vaillancourt, M., 2022. A review on the heat transfer in asphalt pavements and urban heat island mitigation methods. *Construction and Building Materials*, 359, 17.

Son, S., Al-Qadi, I.L., and Zehr, T., 2016. 4.75 mm SMA performance and cost-effectiveness for asphalt thin overlays. *International Journal of Pavement Engineering*, 17, 799–809.

Sun, L., 2016. *Structural behavior of asphalt pavements*.

Sun, T., and Sheng, H., 2020. Heat transfer analysis of microwave hot recycling for asphalt pavement. *Journal of Engineering-Joe*, 2020, 1–5.

Xiao, R., 2022. *Research on Heating Efficiency and Temperature Field Prediction of Hot Air Heating for Asphalt Pavement.* Ph.D. Thesis, Chang'An University.

Xu, X., *et al.*, 2018. Quick heating method of asphalt pavement in hot in-place recycling. *Construction and Building Materials*, 178, 211–218.

Yang, Y., *et al.*, 2012. Bonding characteristics analysis of ultra-thin overlay of asphalt pavement layer. *SUSTAINABLE ENVIRONMENT AND TRANSPORTATION, PTS 1-4*, 178-181, 1245–1249.

Yao, H., *et al.*, 2023. A literature review: Asphalt pavement repair technologies and materials. *Proceedings of the Institution of Civil Engineers: Engineering Sustainability*.

Zhao, X., Shen, A., and Ma, B., 2020. Temperature response of asphalt pavement to low temperatures and large temperature differences. *International Journal of Pavement Engineering*, 21, 49–62.